




Cite this: *Environ. Sci.: Processes Impacts*, 2018, 20, 1007

An experimental methodology to measure the reaction rate constants of processes sensitised by the triplet state of 4-carboxybenzophenone as a proxy of the triplet states of chromophoric dissolved organic matter, under steady-state irradiation conditions†

Marco Minella,^a Lorenzo Rapa,^a Luca Carena,^a Marco Pazzi,^a Valter Maurino,^a Claudio Minero,^a Marcello Brigante^b and Davide Vione ^{*a}

By a combination of transient absorption spectroscopy and steady-state irradiation experiments, we investigated the transformation of phenol and furfuryl alcohol (FFA) sensitised by irradiated 4-carboxybenzophenone (CBBP). The latter is a reasonable proxy molecule to assess the reactivity of the excited triplet states of the chromophoric dissolved organic matter that occurs in natural waters. The main reactive species for the transformation of both phenol and FFA was the CBBP triplet state, despite the fact that FFA is a commonly used probe for ¹O₂. In the case of FFA it was possible to develop a simple kinetic model that fitted well the experimental data obtained by steady-state irradiation, in a wide range of FFA concentration values. In the case of phenol the model was made much more complex by the likely occurrence of back reactions between radical species (e.g., phenoxyl and superoxide). This problem can be tackled by considering only the experimental data at low phenol concentration, where the degradation rate increases linearly with concentration. We do not recommend the use of ¹O₂ scavengers/quenchers such as sodium azide to elucidate CBBP photoreaction pathways, because the azide provides misleading results by also acting as a triplet-state quencher. Based on the experimental data, we propose a methodology for the measurement of the CBBP triplet-sensitisation rate constants from steady-state irradiation experiments, allowing for a better assessment of the triplet-sensitised degradation of emerging contaminants.

Received 5th April 2018
Accepted 8th May 2018

DOI: 10.1039/c8em00155c

rsc.li/espi

Environmental significance

Triplet-sensitised reactions play an important role in the transformation of natural compounds and man-made pollutants in sunlit surface waters. These processes are triggered by the triplet states of chromophoric dissolved organic matter (³CDOM*), but the measurement of ³CDOM* reactivity is a complex task. This task can be simplified by use of proxy molecules for CDOM, where the main difficulty is the paucity of experimental protocols to measure the rate constants of triplet sensitisation with steady-state irradiation experiments. The present paper helps filling this gap.

Introduction

Photochemical processes play an important role in the degradation of biorecalcitrant emerging contaminants in surface waters.¹ These processes involve both direct photolysis and indirect photochemistry induced by photosensitisers, among

which Chromophoric Dissolved Organic Matter (CDOM) usually plays a very important (and sometimes the main) role.² CDOM occurs naturally in surface waters and mostly derives from the degradation of biological materials.^{3,4} The irradiation of CDOM by sunlight triggers the production of a number of reactive transient species such as hydroxyl radicals ([•]OH), singlet oxygen (¹O₂) and CDOM triplet states (³CDOM*).^{5,6} In particular, the triplet states are involved in the degradation of phenols, of several herbicides including phenylureas, of sulfonamide antibiotics, and possibly of additional contaminants of emerging concern (CECs).⁷ A debate has arisen about the importance of aromatic carbonyls and quinones as ³CDOM* sources, with

^aDipartimento di Chimica, Università di Torino, Via Pietro Giuria 5, 10125 Torino, Italy. E-mail: davide.vione@unito.it; Fax: +39-011-6705242; Tel: +39-011-6705296

^bUniversité Clermont Auvergne, CNRS, Sigma Clermont, Institut de Chimie de Clermont-Ferrand, F-63000 Clermont-Ferrand, France

† Electronic supplementary information (ESI) available. See DOI: 10.1039/c8em00155c

recent evidence favouring the former,^{8–11} but single source molecules still escape detection and may additionally vary depending on the CDOM origin, which has been shown to affect the photoreactivity of CDOM itself.¹²

The knowledge of the reaction rate constants between ³CDOM* and CECs would improve the assessment of the role of triplet sensitisation in photodegradation, where the rate constants are used as input data in photochemical models.^{13–15} Unfortunately, because of the complex and still partially unknown structure of CDOM, the nature of ³CDOM* is poorly known as well and this is an obstacle to the assessment of ³CDOM* reactivity toward target contaminants. A possible way out of the problem is the use of proxy molecules for CDOM, which produce triplet states simulating ³CDOM* reactivity.^{16,17} The advantage of using a proxy is that it is easier to assess the reactivity of a triplet state of known nature compared to a mixture of unknown transient species such as ³CDOM*. However, it is important that the proxy shows similar behaviour to CDOM towards triplet sensitisation.

The assessment of triplet-state reactivity faces difficulties even in the case of a well-defined photosensitiser. From an operational point of view, the easiest measurement is that of the quenching rate constants of triplet states by transient absorption spectroscopy through laser flash photolysis (LFP) devices. These measurements are based on the monitoring of the triplet-state decay in the presence of an organic substrate at variable concentration, but they require the availability of a costly laser apparatus and do not distinguish between physical and chemical quenching. Therefore, the rate constant for the quenching of a triplet-state transient by a given substrate is actually an upper limit for the reaction rate constant between the two species.^{18–20} The actual reaction rate constant might be determined in steady-state irradiation experiments, but to do so one needs to know very well the photophysics and photochemistry of the studied system, which usually requires a preliminary study to be carried out by LFP.^{21,22} An additional problem is the possible production of competing transient species such as ¹O₂,²³ which might react with the investigated substrates.

To date a procedure has been available to measure the reaction rate constants with the triplet state of anthraquinone-2-sulphonate (³AQ2S*) under steady-state irradiation,²⁴ following the sufficiently detailed knowledge of the photochemistry and triplet-state chemistry of this compound.²² In some cases the ³AQ2S* rate constants thus determined are representative of the ³CDOM* rate constants they are intended to assess,^{24,25} but it is found quite often that ³AQ2S* is more reactive than typical ³CDOM*.²⁰ The most likely reason is that ³AQ2S* has higher reduction potential than typical ³CDOM* (2.6 V vs. 1.4–1.9 V, respectively).⁷

There is evidence that 4-carboxybenzophenone (CBBP) is a suitable CDOM proxy, because of reasonably comparable reactivity between ³CBBP* and ³CDOM*.²⁰ The likely reason is that the reduction potential of ³CBBP* (1.8 V) is in the range of the ³CDOM* reduction potentials.⁷ Unfortunately, at the moment it is only possible to measure the ³CBBP* quenching rate constants by laser flash photolysis,^{26,27} and no experimental methodology is available to measure the reaction rate constants

in steady-state irradiation experiments. The triplet state ³CBBP* is known to form transient radical-ion pairs with an easily oxidised substrate S after electron abstraction, and these ion pairs partially give back CBBP and S in a photochemically activated null cycle that does not induce transformation.²⁸ This phenomenon causes the ³CBBP* reaction rate constants to be often lower than the corresponding quenching rate constants, and hence it is important to measure the actual ³CBBP* reaction rate constants in steady-state irradiation experiments.

The development of a methodology to measure the ³CBBP* reaction rate constants by steady-state irradiation is the target of the present paper. To do so we initially characterised the ³CBBP* evolution and reactivity by laser flash photolysis, to fill some knowledge gaps that prevent the measurement of the reaction rate constants. The parameters measured by transient absorption spectroscopy are an important basis to compare the results of *ad hoc* steady-state irradiation experiments with the predictions of kinetic models, thereby finding the most suitable level of model complexity and the kind of experimental data that are needed for the measurement of the actual reaction rate constants.

It should be underlined that the main goal here is to find a molecule, the triplet state of which has comparable reactivity to ³CDOM* with xenobiotics, but that does not necessarily reproduce the photochemical behaviour of CDOM in all the other respects. In other words, the ideal ³CDOM* proxy (a terminology that should be preferred in this context over that of the “CDOM proxy”) should have the following features: (i) its triplet state should react with xenobiotics in a similar way to typical ³CDOM*; (ii) it should not produce interfering transient species under irradiation. Such species are actually produced by irradiated CDOM, but they may provide biased results in the context of the measurement of the ³CDOM* rate constants; and (iii) it should allow for the measurement of the triplet-sensitisation reaction rate constants by means of steady-state irradiation experiments. It is notable that AQ2S performed well in the last two points but not in the first one, while a compound that reproduced the photochemical CDOM behaviour in all of its respects (including the photochemical generation of interfering species) might be problematic as far as points (ii, iii) are concerned.

Methods

All the used chemicals were of analytical grade (gradient grade in the case of eluents for liquid chromatography) and they were used as received, without further purification. Furfuryl alcohol (FFA, 98% purity, Aldrich) was purchased in the smallest amount available (50 g) and used soon after delivery, to limit degradation that occurs even under refrigeration with eventual formation of coloured compounds. This issue is confirmed by the detection in the stock solutions of small amounts of furfural as an FFA oxidation intermediate (*vide infra*), although the same solutions did not significantly absorb radiation above 400 nm. Moreover, the absence of FFA direct photolysis (which could possibly be induced by light-absorbing impurities) was checked prior to the relevant experiments. Water was of Milli-Q quality

(resistivity > 18 M Ω cm, organic carbon < 2 ppb). To keep CBBP in the deprotonated form ($pK_a \sim 4.5$),²⁹ NaOH was used to adjust the pH of the solutions to ~ 7 . The pH values were measured with a combined glass electrode connected to a Met-rohm 602 pH meter.

Laser flash photolysis (LFP) experiments

The reactivity of ³CBBP* was studied using the fourth harmonic (266 nm) of a Quanta Ray GCR 130-01 Nd:YAG laser system instrument, used in a right-angle geometry with respect to the monitoring light beam. The single pulses energy was set to 35–40 mJ. A 3 mL solution volume containing 100 $\mu\text{mol L}^{-1}$ CBBP in H₂O at pH ~ 7 was placed into a quartz cuvette (path length of 1 cm) and used for a maximum of four consecutive laser shots, to avoid interference by phototransformation products. Where applicable, the solution also contained variable concentrations of ³CBBP* quenchers such as phenol, furfuryl alcohol (FFA) or NaN₃. In a further series of experiments, solutions containing 100 $\mu\text{mol L}^{-1}$ CBBP alone were preliminarily purged with high-purity Ar or O₂ for 10 min to obtain deoxygenated or fully oxygenated conditions. During the relevant LFP measurements a gentle gas flow was maintained above the cuvette, to avoid air dissolution while not perturbing the aqueous phase with gas bubbles. The absorbance of ³CBBP* at its 550 nm absorption peak was monitored over time by using a detection system consisting of a pulsed xenon lamp (150 W), a monochromator and a photomultiplier (1P28). A spectrometer control unit was used for synchronising the pulsed light source and programmable shutters with the laser output. The signal from the photomultiplier was digitised by using a programmable digital oscilloscope (HP54522A). A 32 bit RISC-processor kinetic spectrometer workstation was used to analyse the digitised signal.

The decay of ³CBBP* was monitored at different concentrations of the added quenchers, and the measured pseudo-first order decay constant k_{CBBP^*} was reported as a function of the quencher concentration. The slopes of the linearly fitted data of k_{CBBP^*} vs. [quencher] were used to obtain the second-order quenching rate constants of ³CBBP* by phenol, FFA, N₃⁻ and O₂ (Stern–Volmer approach).

Steady-state irradiation experiments

The solutions to be irradiated (air-saturated, 5 mL total water volume, pH ~ 7 by NaOH) were placed in cylindrical Pyrex glass cells equipped with a lateral neck for sample transfer, which was tightly closed with a screw cap. The cells were placed under a 40 W Philips TL-K 05 lamp, having an emission maximum at 365 nm and producing a UV irradiance of 21 W m⁻² on top of the irradiated solutions. The UV irradiance (290–400 nm) was measured with an irradiance meter by CO.FO.ME.GRA. (Milan, Italy). The optical path length within the irradiated solutions was 0.4 cm. The lamp emission spectrum was taken with a calibrated Ocean Optics USB 2000 CCD spectrophotometer and corrected for the transmittance of the Pyrex window of the irradiation cells. Based on these data, the actual spectral photon flux density of the lamp was obtained by chemical actinometry

using 2-nitrobenzaldehyde (NBA). The detailed procedure for NBA actinometry is described elsewhere.³⁰ The lamp spectral photon flux density thus obtained is reported in Fig. 1, together with the absorption spectrum (molar absorption coefficient) of CBBP. The latter was measured with a Varian Cary 100 Scan double-beam UV-visible spectrophotometer, using Hellma quartz cuvettes with a 1 cm optical path length.

After the scheduled irradiation time, the cells were withdrawn from the lamp and the contents were analysed by high-performance liquid chromatography coupled with diode-array detection (HPLC-DAD). The used instrument was a VWR-Hitachi LaChrom Elite chromatograph equipped with an L-2200 autosampler (injection volume 60 μL), L-2130 quaternary pump for low-pressure gradients, Duratec vacuum degasser, L-2300 column oven (set at 40 $^{\circ}\text{C}$), and L-2455 photodiode array detector. The column was a VWR LiChroCART 125-4 Cartridge, packed with LiChrospher 100 RP-18 (125 mm \times 4 mm \times 5 μm). Elutions were carried out at a 1.0 mL min⁻¹ flow rate using the eluents A = aqueous H₃PO₄ at pH 2.8 and B = methanol. Phenol and CBBP were monitored with the following step gradient: 40% A for 6 min and then to 70% A in 0.1 min and kept for 6 min, and down to 40% A in 0.1 min and kept for 6 min (post-run equilibration). Under these conditions the retention times were 3.7 min for phenol, quantified at 220 nm, and 10.6 min for CBBP, quantified at 265 nm. In the case of the monitoring of FFA and CBBP the following linear gradient was used: 15% A for 2.5 min, and then to 70% A reached at 4.0 min and kept till 10.0 min, and finally down to 15% A reached at 12.0 min and kept till 16.0 min (post-run equilibration). The retention times were 4.3 min for FFA, quantified at 220 nm, and 8.8 min for CBBP, quantified at 265 nm.

The time trends of phenol and FFA were fitted with an exponential function with a residual, namely $C_t/C_o = 1 + A(e^{-kt} - 1)$, where C_t is the concentration of the compound at the time t , C_o its initial concentration, k the pseudo-first order decay constant, and A fit parameter. The need to introduce the residual in the fit function was motivated by a loss of reactivity of the studied systems at relatively long irradiation times.

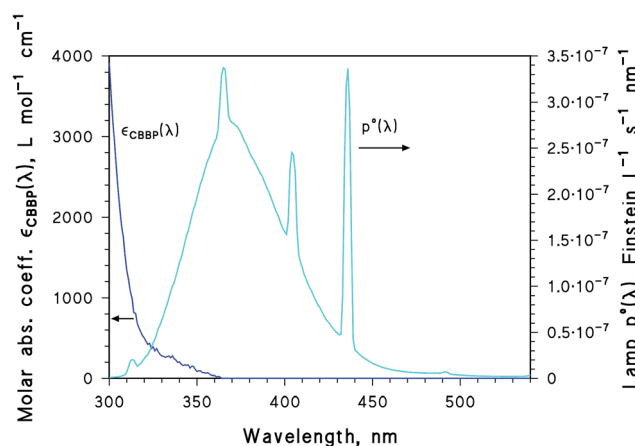


Fig. 1 Molar absorption coefficient $\epsilon(\lambda)$ of CBBP and emission spectrum (spectral photon flux density $p^\circ(\lambda)$) of the used irradiation system (Philips TL-K 05 lamp).

Considering that CBBP underwent relatively limited degradation, the most likely explanation is interference (*e.g.*, reduction of partially oxidised substrates back to the parent compound) caused by transformation intermediates of CBBP, phenol or FFA. The initial degradation rate was calculated as $R_0 = kAC_0$. The error bounds associated with the rate data represent the (σ -level, 66% confidence interval) intra-series variability between the experimental data and the fit function (*i.e.*, the goodness of the fit). Data fit, fit uncertainty estimations and data plots were determined with FigP software (Biosoft, Cambridge, UK). The original plots were exported into .cgm format and then converted into .jpg by using Microsoft Power Point (PPT). To avoid the loss of resolution in the .jpg files, the PPT presentation size was set at 120 × 90 cm. The error in reproducibility between experimental replicas (inter-series variability, obtained by repeating some of the experiments twice) was in the order of <20%.

Experiments with D₂O. This series of experiments was carried out to quantify the importance of ¹O₂ in the photo-degradation of FFA sensitised by CBBP, exploiting the fact that the lifetime of ¹O₂ in D₂O is 12.5 times longer than that in H₂O.³¹ The solution of CBBP in D₂O was prepared by dissolving 4 mg CBBP in 20 mL D₂O, together with NaH₂PO₄ + Na₂HPO₄ (mixture of the two solids, total concentration 24 mmol L⁻¹) to achieve pH ~ 7. The suspension was stirred for one day inside a closed vial to maximise CBBP dissolution, and then it was filtered (0.45 μm hydrophilic PVDF filter membranes, Millex – Merck Millipore) and the concentration of CBBP (83 μmol L⁻¹) was determined by absorption spectroscopy at 300 nm. At the same time a 24 mmol L⁻¹ solution of FFA in D₂O was prepared, 21 μL of which were mixed inside each irradiation cell together with 5 mL of the 83 μmol L⁻¹ CBBP solution described above. The final FFA concentration inside each cell was 0.1 mmol L⁻¹. The phosphate buffer (NaH₂PO₄ + Na₂HPO₄) could contribute some H atoms to the system, but at most one would obtain 0.03% H₂O and 99.97% D₂O. After irradiation, the time trend of FFA was monitored by HPLC as described above.

The D₂O experiments were compared with analogous irradiation experiments carried out in H₂O with 83 μmol L⁻¹ CBBP + 1 mmol L⁻¹ FFA, at pH ~ 7 adjusted with 24 mmol L⁻¹ NaH₂PO₄ + Na₂HPO₄. Moreover, to check (and eventually exclude) the possible effect of the phosphate buffer on FFA degradation, additional experiments were carried out in H₂O in the presence of 83 μmol L⁻¹ CBBP + 1 mmol L⁻¹ FFA, at pH ~ 7 adjusted with NaOH. In the latter case, a 0.1 mmol L⁻¹ CBBP solution in H₂O was titrated with a NaOH solution till pH 7 (checked with a pH meter), and then it was transferred into a 100 mL volumetric flask and brought to volume by adding both H₂O and a stock FFA solution. The final concentration values were 83 μmol L⁻¹ CBBP and 1 mmol L⁻¹ FFA, and this solution was transferred into the irradiation cells for the irradiation experiments.

Identification of transformation intermediates

To identify the transformation intermediates of phenol and CBBP, 15 mL solutions were irradiated for 0, 4, 8 and 16 hours. After the scheduled irradiation times, the solutions were placed

in cylindrical vials, acidified with HCl to pH ~ 1, salted with NaCl, and extracted in sequence with 3 aliquots of 2 mL dichloromethane each. The dichloromethane extracts were then combined and subsequently concentrated under a nitrogen stream to ~200 μL. The extracts were then analysed by gas chromatography-mass spectrometry (GC-MS). The instrument (Agilent 6890, series II) was equipped with a 5% phenylmethylpolysiloxane column (Agilent HP-5ms; 30 m × 0.25 mm). The GC operating parameters were as follows: injector at 300 °C, pulsed splitless injection (20 psi, 1 min), volume injected 1 μL, and constant He carrier flow (1 mL min⁻¹). The analyses were performed using the following temperature gradient: after an initial 3 minutes at 40 °C, the temperature was linearly increased at 7 °C min⁻¹ from 40 to 300 °C and then kept at 300 °C for 10 min. The ionisation interface worked in the electron impact (EI) mode at 70 eV. Under these conditions, the retention times verified by injection of dichloromethane solutions of authentic standards were (min): phenol (13.5), CBBP (41.7), 2,2'-dihydroxybiphenyl (32.4), 4,4'-dihydroxybiphenyl (40.2) and 4-phenoxyphenol (34.0). The intermediate identification was obtained by examining the mass spectra and by using library matching (NIST 02 and Wiley 275).

To identify the transformation intermediates of FFA and CBBP, 5 mL solutions were irradiated for 0, 4, 8 and 16 hours, and then placed in cylindrical vials closed with septum screw caps, amended with ~2 g of NaCl and thermostated at 40 °C. A SPME fibre coated with Carboxen-PDMS (75 μm thickness; Supelco Co.) was preconditioned at 300 °C for 60 min, inserted into the sample vial through the septum and then exposed to the head-space for 15 min under constant stirring. Thereafter, the SPME fibre was inserted into the injector of a gas chromatograph and it underwent desorption for 5 min at 280 °C. In this case the instrument was equipped with a 6%-cyanopropylphenyl-94%-dimethylpolysiloxane column (Zebron ZB-624; 30 m × 0.25 mm × 1.40 μm). The injector was kept at 280 °C using splitless injection (7.47 psi), and a constant He carrier flow (1 mL min⁻¹) was used, as well as the following temperature gradient: after an initial 5 minutes at 40 °C, the temperature was linearly increased at 15 °C min⁻¹ from 40 to 260 °C and then kept at 260 °C for 2.33 min. The ionisation interface worked in the electron impact (EI) mode at 70 eV and 230 °C, while the temperature of the quadrupole was set at 150 °C. A solvent delay of 2.80 min was used to avoid the overloading of the detector. Under these conditions, the retention time of FFA was 12.3 min and that of furfural was 11.9 min.

Results and discussion

Laser flash photolysis (LFP) experiments

The reactivity of ³CBBP* was first studied by means of quenching experiments carried out with the LFP technique at pH ~ 7. A 266 nm laser pulse excites CBBP to the singlet state, after which inter-system crossing (ISC) to ³CBBP* takes place. In the case of CBBP the ISC is known to be very effective, with a quantum yield $\Phi_{ISC} \sim 1$,³² and thus practically every photon absorbed yields ³CBBP*. The pseudo-first order rate constant of

$^3\text{CBBP}^*$ decay ($k_{^3\text{CBBP}^*}$) was measured as a function of the concentration values of relevant dissolved species, including oxygen, phenol, furfuryl alcohol (FFA) and sodium azide (NaN_3). A linear increase of $k_{^3\text{CBBP}^*}$ as a function of the quencher concentration was found, which allowed for the determination of the quenching rate constants reported in Table 1. An example of raw LFP data is reported in Fig. ESI1 in the ESI.† The linear plots are reported in Fig. ESI2 (ESI†). The rate constant between $^3\text{CBBP}^*$ and ground-state CBBP ($5 \times 10^6 \text{ L mol}^{-1} \text{ s}^{-1}$)²⁷ is sufficiently low to ensure that this process only accounted for a negligible fraction of the observed $^3\text{CBBP}^*$ decay in the presence of $100 \mu\text{mol L}^{-1}$ CBBP.

First of all the experimental data showed that the value of $k_{^3\text{CBBP}^*}$ was significantly lower in deoxygenated than in aerated solution (where $[\text{O}_2] = 0.3 \text{ mmol L}^{-1}$), which suggests a significant deactivation of $^3\text{CBBP}^*$ by oxygen. By comparing the decay kinetics under the two conditions, one gets that in aerated solution about 32% of $^3\text{CBBP}^*$ would undergo O_2 -independent quenching (e.g., internal conversion), and the remaining 68% would react with dissolved O_2 . Note that the $^3\text{CBBP}^*$ decay in aerated solution, with a rate constant around $6 \times 10^5 \text{ s}^{-1}$, was comparable to data reported in the literature.^{17,33} The reaction between $^3\text{CBBP}^*$ and O_2 may potentially give $^1\text{O}_2$, but the production of CBBP and O_2 can also take place.³⁴ Given the unity quantum yield for $^3\text{CBBP}^*$ production from light-excited CBBP ($\Phi_{^3\text{CBBP}^*}^{\text{CBBP}} \approx 1$), one gets an upper limit of 0.68 for the formation quantum yield of $^1\text{O}_2$ by light-excited CBBP in aerated solution, where 68% $^3\text{CBBP}^*$ is scavenged by O_2 ($\Phi_{^1\text{O}_2}^{\text{CBBP}} \leq 0.68 \Phi_{^3\text{CBBP}^*}^{\text{CBBP}}$). The actual value of $\Phi_{^1\text{O}_2}^{\text{CBBP}}$ is most likely lower, because the triplet states of aromatic carbonyls are known to produce $^1\text{O}_2$ with yields $S_\Delta < 1$ upon reaction with molecular oxygen (it is reported, e.g., $S_\Delta = 0.29$ for benzophenone and 0.5 for 2-acetonaphthone).^{34,35}

The excited state $^3\text{CBBP}^*$ is significantly quenched by phenol and, most notably, by FFA and N_3^- (see Table 1). Interestingly, $^3\text{CBBP}^*$ is quenched with rate constants above $10^9 \text{ L mol}^{-1} \text{ s}^{-1}$ by molecules such as FFA and N_3^- , which are often used as $^1\text{O}_2$ quenchers.^{36–38} A similar finding has already been reported for $^3\text{AQ2S}^*$ (the measured rate constants were, respectively, $k_{^3\text{AQ2S}^*,\text{FFA}} \geq 4 \times 10^9 \text{ L mol}^{-1} \text{ s}^{-1}$ and $k_{^3\text{AQ2S}^*,\text{N}_3^-} = 4.4 \times 10^9 \text{ L mol}^{-1} \text{ s}^{-1}$).²¹ This finding is reasonable when considering that the reduction potentials of the radicals derived from the one-electron oxidation of FFA and N_3^-

are 0.9 and 1.3 V, respectively.^{39,40} Most importantly, we suggest that the mere addition of scavengers/quenchers to assess reaction mechanisms may provide biased results if the unintended additional reactivity is not taken into account. The bias arises from the wrong assumption that the added compounds quench selectively the target transient species, $^1\text{O}_2$ in this case.

The quenching rate constants obtained by LFP are upper limits for the reaction rate constants that can be derived from steady-state irradiation experiments.²⁸ Although a quenching phenomenon may not lead to chemical reactivity, its rate constant is needed to calculate the steady-state concentration of $^3\text{CBBP}^*$ in the presence of the quencher.

Steady-state irradiation experiments

Phenol photodegradation. The rate of phenol degradation sensitised by $^3\text{CBBP}^*$ was measured as a function of phenol concentration. The initial CBBP concentration was set at $66 \mu\text{mol L}^{-1}$ and the initial pH was adjusted to ~ 7 . Under these conditions the photon flux absorbed by CBBP, which is the only light-absorbing species in the system, can be calculated as⁴¹ $P_a^{\text{CBBP}} = \int_{\lambda} p^\circ(\lambda)[1 - 10^{-A_{\text{CBBP}}(\lambda)}]d\lambda = 5.8 \times 10^{-8} \text{ Ein L}^{-1} \text{ s}^{-1}$, where $p^\circ(\lambda)$ is the lamp photon flux density and $A_{\text{CBBP}}(\lambda)$ is the absorbance of $66 \mu\text{mol L}^{-1}$ CBBP. Because CBBP has a unity quantum yield of inter-system crossing,³² the $^3\text{CBBP}^*$ formation rate can be calculated as $R_{^3\text{CBBP}^*} = P_a^{\text{CBBP}} = 5.8 \times 10^{-8} \text{ mol L}^{-1} \text{ s}^{-1}$. The trend of the initial degradation rate of phenol (R_{phenol}) as a function of phenol concentration is provided in Fig. 2. From the figure one can see an initially linear increase of R_{phenol} vs. $[\text{phenol}]$ (up to approximately $20 \mu\text{mol L}^{-1}$ phenol, see

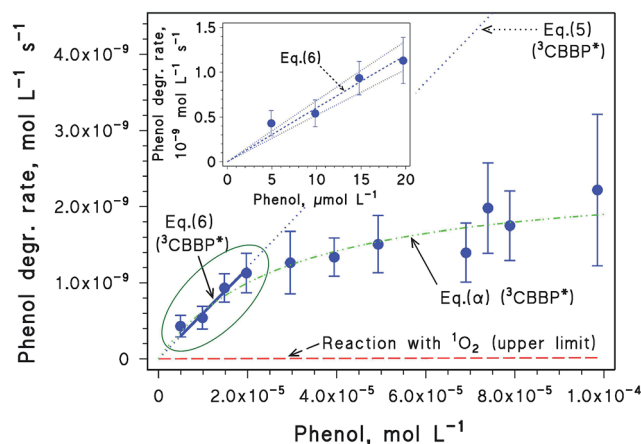


Fig. 2 Initial degradation rate of phenol (R_{phenol}) as a function of phenol concentration, upon irradiation in the presence of $66 \mu\text{mol L}^{-1}$ CBBP at pH ~ 7 . The error bounds to the rate values ($\pm\sigma$) are derived from the fit of the time evolution data of phenol concentration. The solid blue line represents the fit of the experimental data (linear tract) with eqn (6), prolonged as the blue dotted curve according to eqn (5). The dash-dotted green curve represents the fit of the experimental data with eqn (α) (see Scheme 1). The dashed red line is the predicted upper limit for the reaction rate between phenol and $^1\text{O}_2$. The inset figure shows a detail of the linear trend, including the fit with eqn (6) (dashed) and the 95% confidence bands of the fit (dotted).

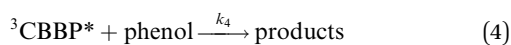
Table 1 First-order decay or second-order quenching constants of $^3\text{CBBP}^*$ determined by laser flash photolysis experiments. The decay constant $k_{^3\text{CBBP}^*,\Delta}$ represents the decay of $^3\text{CBBP}^*$ in the absence of dissolved O_2 (it is $k_{^3\text{CBBP}^*,\Delta} = 0.32k_2$). The Stern–Volmer plots relative to O_2 , phenol, FFA and N_3^- are reported in the ESI

Rate constant	Numerical value (66% confidence level, σ -level uncertainty)
$k_{^3\text{CBBP}^*,\Delta}, \text{ s}^{-1}$	$(2.0 \pm 0.1) \times 10^5$
$k_{^3\text{CBBP}^*,\text{O}_2}, \text{ L mol}^{-1} \text{ s}^{-1}$	$(1.3 \pm 0.1) \times 10^9$
$k_{^3\text{CBBP}^*,\text{phenol}}, \text{ L mol}^{-1} \text{ s}^{-1}$	$(8.9 \pm 0.9) \times 10^8$
$k_{^3\text{CBBP}^*,\text{FFA}}, \text{ L mol}^{-1} \text{ s}^{-1}$	$(2.35 \pm 0.08) \times 10^9$
$k_{^3\text{CBBP}^*,\text{N}_3^-}, \text{ L mol}^{-1} \text{ s}^{-1}$	$(2.35 \pm 0.05) \times 10^9$

details in the figure inset), followed by a plateau trend. The plateau is located at $R_{\text{phenol}} \sim 2 \times 10^{-9} \text{ mol L}^{-1} \text{ s}^{-1}$, which is considerably lower than the R_{CBBP^*} value assessed above.

The significant involvement of $^1\text{O}_2$ in phenol degradation was excluded by considering an upper limit for the transformation of phenol by $^1\text{O}_2$. In this simplified approach we assumed: (i) formation of $^1\text{O}_2$ with $\phi_{^1\text{O}_2}^{\text{CBBP}^*} = 0.68$ (upper limit); (ii) reaction between $^1\text{O}_2$ and phenol with $k_{^1\text{O}_2, \text{phenol}} = 2.6 \times 10^6 \text{ L mol}^{-1} \text{ s}^{-1}$,^{42,43} and (iii) deactivation of $^1\text{O}_2$ by collision with the solvent ($k_d = 2.5 \times 10^5 \text{ s}^{-1}$).⁴⁴ The quenching of $^3\text{CBBP}^*$ by phenol, which would lead to a decrease of $\phi_{^1\text{O}_2}^{\text{CBBP}^*}$, was neglected. The calculation results are provided in Fig. 2 and they show that, even with an upper limit for $\phi_{^1\text{O}_2}^{\text{CBBP}^*}$, the reaction between phenol and $^1\text{O}_2$ was totally negligible.

The linear portion of R_{phenol} vs. [phenol] can be interpreted in the framework of a kinetic model where $^3\text{CBBP}^*$ is generated by CBBP irradiation and it is quenched by internal conversion and by interaction with O_2 and with phenol. The latter process would at least in part induce phenol degradation. In the kinetic model, the reaction rate constant between $^3\text{CBBP}^*$ and phenol was allowed to be different from (*i.e.*, lower than) the quenching rate constant measured by LFP. The following kinetic scheme was used:



In the above scheme the inactivation rate constant $k_2 = 6 \times 10^5 \text{ s}^{-1}$, determined as the average decay constant of $^3\text{CBBP}^*$ in aerated solution in the absence of quenchers (see ESI†), takes into account both $^3\text{CBBP}^*$ internal conversion and quenching by oxygen under aerated conditions. Moreover, reaction (3) (which also includes (4)) was used to determine the decay of $^3\text{CBBP}^*$, and reaction (4) to compute the degradation rate of phenol. We used $k_3 = 8.9 \times 10^8 \text{ L mol}^{-1} \text{ s}^{-1}$ (determined by LFP) as the value of the $^3\text{CBBP}^*$ quenching rate constant by phenol. By applying the steady-state approximation to $^3\text{CBBP}^*$ we got the following expression for R_{phenol} , where $R_{\text{CBBP}^*} = 5.8 \times 10^{-8} \text{ mol L}^{-1} \text{ s}^{-1}$ as per the above discussion and k_4 was the only free-floating fit parameter:

$$R_{\text{phenol}} = R_{\text{CBBP}^*} \frac{k_4[\text{phenol}]}{k_2 + k_3[\text{phenol}]} \quad (5)$$

The fit of the experimental data with eqn (5) is reported in Fig. 2 (see the main figure and inset), but only the initial linear part of R_{phenol} vs. [phenol] could be fitted conveniently. In the linear part, the fit function reduces to the following:

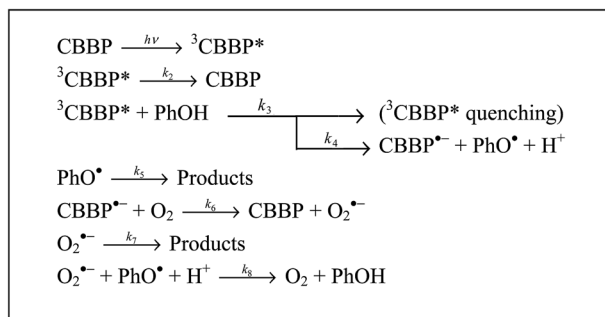
$$R_{\text{phenol}} = R_{\text{CBBP}^*} k_4 k_2^{-1} [\text{phenol}] \quad (6)$$

In the latter case the fit yielded $k_4 = (6.4 \pm 0.3) \times 10^8 \text{ L mol}^{-1} \text{ s}^{-1}$ that is $\sim 30\%$ lower than k_3 . This finding is reasonable because $^3\text{CBBP}^*$ is known to form short-lived radical ion pairs with dissolved substrates, leading to partial relaxation back to the initial ground-state compounds.²⁸ The linearity of the experimental data that allowed for a good fit with eqn (6) ($[\text{phenol}] \leq 20 \mu\text{mol L}^{-1}$) suggests that $k_3[\text{phenol}]$ was lower than k_2 . Coherently, from the LFP results one gets that $k_3[\text{phenol}] \leq 0.03 \times k_2$ if $[\text{phenol}] \leq 20 \mu\text{mol L}^{-1}$.

Eqn (5) assumes competition between $^3\text{CBBP}^*$ decay and quenching by phenol (reactions (2) and (3), respectively), the kinetics of which is obtained by LFP experiments. The prolongation of eqn (5) beyond the linear range is reported as the dotted curve in Fig. 2, and it clearly shows that the assumed competition was unable to account for the observed plateau trend of the experimental data. Indeed, eqn (5) foresees a plateau if $k_3[\text{phenol}] > k_2$, but this condition requires $[\text{phenol}] > 0.7 \text{ mmol L}^{-1}$ while the experimental data suggest a plateau for phenol concentration values that are at least ten times lower than that.

To account for the plateau, one has to hypothesise additional reactions that would become important at high phenol concentration values. One such possibility is the back-reaction between radical species formed in reaction (4) and/or in later processes. Such a hypothesis looks reasonable because, with increasing phenol concentration, a growing fraction of $^3\text{CBBP}^*$ would be scavenged by phenol itself, increasing the formation rates of the radical species and, as a consequence, also the likelihood of radical-radical recombination.⁴⁵ The inclusion in the kinetic model of the most straightforward recombination process, namely that between phenoxyl and the ketyl radical/ketyl radical anion of CBBP (the CBBP ketyl radical has $\text{p}K_a = 8.2$),²⁸ introduces quadratic terms in the steady-state kinetic calculations and prevents obtaining a manageable rate equation. In contrast, by assuming recombination between phenoxyl and superoxide^{46–48} (see Scheme 1) one gets a manageable though complex equation (eqn (α) in Scheme 1) that fits the experimental data rather well (see Fig. 2). Unfortunately eqn (α) is not suitable to obtain meaningful numerical values by data fitting, for two reasons: (i) important approximations were made to obtain it (the recombination reactions involving phenoxyl + phenoxyl and superoxide + hydroperoxide were approximated as pseudo-first order processes to avoid quadratic terms and, with the same purpose, the reaction between phenoxyl and superoxide was assumed not to affect significantly the steady-state $[\text{O}_2^{\cdot-}]$), and (ii) eqn (α) is very complex, and the unknown parameters to be obtained by data fitting are not all orthogonal; this issue introduces important uncertainties in the relevant numerical values.

To prove the actual formation of phenoxyl in the studied system, phenol dimers including phenoxyphenols and dihydroxybiphenyls were identified by CH_2Cl_2 extraction and GC-MS analysis. These compounds are in fact well known to be formed upon dimerisation of phenoxyl.^{46–48} In particular, the formation of 2,2'-dihydroxybiphenyl, 4,4'-dihydroxybiphenyl and 4-phenoxyphenol upon irradiation of CBBP and phenol was demonstrated by comparison with authentic standards. Furthermore,



$$R_{\text{phenol}} = \left(\frac{R_{{}^3\text{CBBP}^*} k_4 [\text{Phenol}]}{k_2 + k_3 [\text{Phenol}]} \right) \left(1 - \frac{R_{{}^3\text{CBBP}^*} k_4 k_8 [\text{Phenol}]}{k_7 (k_2 + k_3 [\text{Phenol}]) \left(k_5 + \frac{R_{{}^3\text{CBBP}^*} k_4 k_8 [\text{Phenol}]}{k_7 (k_2 + k_3 [\text{Phenol}])} \right)} \right) \quad (\text{Eq. } \alpha)$$

Scheme 1 Kinetic scheme of the reaction process that hypothesises radical–radical recombination between phenoxyl (PhO^{\bullet}) and superoxide ($\text{O}_2^{\bullet-}$). Eqn (α) was obtained upon application of the steady-state approximation to ${}^3\text{CBBP}^*$, $\text{CBBP}^{\bullet-}$, PhO^{\bullet} and $\text{O}_2^{\bullet-}$. Note that the decay of PhO^{\bullet} and $\text{O}_2^{\bullet-}$ is here assumed to be a pseudo-first-order process described by the rate constants k_5 and k_7 , which allows for non-manageable quadratic terms to be avoided. However, the decay of the two radical species is much more likely to involve second-order reactions ($\text{PhO}^{\bullet} + \text{PhO}^{\bullet}$ and $\text{O}_2^{\bullet-} + \text{HO}_2^{\bullet}$, respectively). Finally, always with the purpose of avoiding quadratic terms, the reaction between PhO^{\bullet} and $\text{O}_2^{\bullet-}$ was assumed not to affect significantly the decay of $\text{O}_2^{\bullet-}$.

two additional dimeric species were tentatively identified as 2,4'-dihydroxybiphenyl and 2-phenoxyphenol. A sample GC-MS chromatogram is provided in the ESI as Fig. ESI3,[†] while Fig. ESI4–7[†] show the relevant mass spectra.

An important reaction between phenol and ${}^1\text{O}_2$ could be excluded here, because the photochemistry of CBBP was known well enough from literature data and from our LFP experiments. However, in many cases one does not have such an abundance of information. The use of quenchers/scavengers has become quite popular to get mechanistic insights into photochemical reactions, including the possible involvement of ${}^1\text{O}_2$ in photodegradation pathways that are known in much less detail when compared to the CBBP/phenol system. This system is sufficiently well understood to allow for a check on the possible conclusions that might be obtained from the use of quenchers/scavengers. NaN_3 is often used as a ${}^1\text{O}_2$ quencher, and here we tested the often-assumed hypothesis that it quenches ${}^1\text{O}_2$ selectively. The experimental trend of R_{phenol} ($C_0 = 0.1 \text{ mmol L}^{-1}$) with irradiated $66 \mu\text{mol L}^{-1}$ CBBP as a function of the azide concentration is reported in Fig. 3. At first sight, one might conclude that ${}^1\text{O}_2$ plays a significant role in phenol degradation because the process is inhibited by azide addition (phenol degradation rate was decreased by about four times with 0.8 mM azide when compared to no azide). From the above discussion we know that this is not true, however, and the quenching of ${}^3\text{CBBP}^*$ by azide should rather be invoked to account for the decrease of the phenol degradation rate. Anyway, a merely qualitative approach to the azide addition procedure might easily provide misleading results.

As an alternative, one could make a more quantitative check and see whether the effect of azide addition is consistent with a ${}^1\text{O}_2$ -induced reaction. To do so, one needs to consider ${}^1\text{O}_2$

consumption by collisional deactivation ($k_d = 2.5 \times 10^5 \text{ s}^{-1}$),⁴⁴ quenching by azide (with a rate constant $k_{\text{tO}_2, \text{N}_3^-} = 5 \times 10^8 \text{ L mol}^{-1} \text{ s}^{-1}$),⁴⁹ and reaction with phenol (with $k_{\text{tO}_2, \text{phenol}} = 2.6 \times 10^6 \text{ L mol}^{-1} \text{ s}^{-1}$).^{42,43} Here we did not try to quantify $R_{{}^3\text{CBBP}^*}$ from $\Phi_{{}^1\text{O}_2}^{\text{CBBP}}$ and F_a^{CBBP} , as done beforehand, because this piece of information is often not available for photosensitisers different from CBBP. We rather assumed that

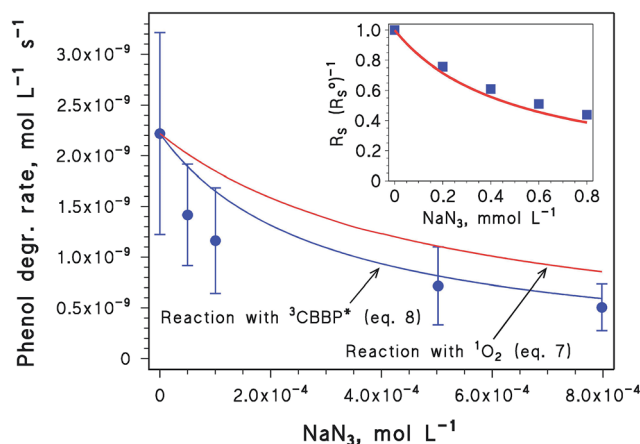


Fig. 3 Initial degradation rate of 0.1 mmol L^{-1} phenol (R_{phenol}) as a function of the concentration of added NaN_3 , upon irradiation in the presence of $66 \mu\text{mol L}^{-1}$ CBBP at $\text{pH} \sim 7$. The error bounds to the rate values ($\pm\sigma$) are derived from the fit of the time evolution data of phenol concentration. The two curves represent the reproduction of the experimental data with eqn (7) and (8). In the inset figure, the solid squares represent the hypothetical behaviour of a compound S having $k_{\text{tO}_2, \text{S}} = 2.6 \times 10^7 \text{ L mol}^{-1} \text{ s}^{-1}$ and $k_{{}^3\text{CBBP}^*, \text{S}} = 8.9 \times 10^9 \text{ L mol}^{-1} \text{ s}^{-1}$ (i.e., ten times more reactive than phenol with both ${}^1\text{O}_2$ and ${}^3\text{CBBP}^*$), and reacting almost exclusively with ${}^3\text{CBBP}^*$. The solid curve represents the predicted trend of $R_{{}^3\text{CBBP}^*} / (R_{{}^3\text{CBBP}^*}^0)^{-1}$ vs. $[\text{N}_3^-]$, if ${}^1\text{O}_2$ is assumed to be the prevailing reactive transient species in the system.

$R_{\text{phenol}} = R_{\text{phenol}}^{\circ} \alpha$, where α is the ratio between the $^1\text{O}_2$ -induced reaction rates in the presence (R_{phenol}) and absence ($R_{\text{phenol}}^{\circ}$) of the azide. The α parameter was evaluated by applying the steady state approximation to $^1\text{O}_2$, under the hypothesis that phenol is mainly transformed by reaction with $^1\text{O}_2$. With this approach one gets the following equation for the effect of added azide on R_{phenol} (note that the equation has no free-floating parameters):

$$R_{\text{phenol}} = R_{\text{phenol}}^{\circ} \frac{k_d + k_{1\text{O}_2, \text{phenol}}[\text{phenol}]}{k_d + k_{1\text{O}_2, \text{phenol}}[\text{phenol}] + k_{1\text{O}_2, \text{N}_3^-}[\text{N}_3^-]} \quad (7)$$

The relevant trend reported in Fig. 3 shows that the $^1\text{O}_2$ hypothesis does not account well for the experimental data: the $^1\text{O}_2$ reaction curve is not included in the σ -level (66% significance) error bars of the experimental rates, although it is a rather narrow miss. In other words, an important involvement of $^1\text{O}_2$ in phenol degradation could be narrowly excluded with this approach at the 66% confidence level (however, given the large error bar on $R_{\text{phenol}}^{\circ}$, one could produce a trend described by eqn (7) that accounts well for the azide data and is still compatible with the experimental $R_{\text{phenol}}^{\circ}$). Differently from a merely qualitative approach, kinetic modelling might have some chance to correctly question the involvement of $^1\text{O}_2$ in phenol degradation. Nevertheless, if one uses (as often done) a 95% confidence level where the error bars to the experimental data are almost twice higher, the scenario becomes less straightforward.

From the results of previous experiments, we actually know that the effect of the azide on R_{phenol} is the consequence of competition between phenol and azide itself for $^3\text{CBBP}^*$. By considering reactions (1)–(4) plus the quenching of $^3\text{CBBP}^*$ by N_3^- , with a rate constant $k_{3\text{CBBP}^*, \text{N}_3^-} = 2.4 \times 10^9 \text{ L mol}^{-1} \text{ s}^{-1}$ as per our LFP results (see Table 1), and by applying a similar approach to that for eqn (7) one gets the following:

$$R_{\text{phenol}} = R_{\text{phenol}}^{\circ} \frac{k_2 + k_3[\text{phenol}]}{k_2 + k_3[\text{phenol}] + k_{3\text{CBBP}^*, \text{N}_3^-}[\text{N}_3^-]} \quad (8)$$

Eqn (8) does not contain k_4 , which is included in $R_{\text{phenol}}^{\circ}$. As shown in Fig. 3, eqn (8) accounts reasonably well for the experimental data, but the $^3\text{CBBP}^*$ curve (eqn (8)) and the $^1\text{O}_2$ one (eqn (7)) are not very distant. Indeed, the exclusion of the $^1\text{O}_2$ process might not be possible for all compounds. A hypothetical compound S, reacting ten times faster than phenol with both $^3\text{CBBP}^*$ and $^1\text{O}_2$, would again undergo degradation almost exclusively by reaction with $^3\text{CBBP}^*$. Competition between S and N_3^- for reaction with $^3\text{CBBP}^*$ affords the use of the equivalent of eqn (8), with S in place of phenol and k_3 increased by ten times, to produce the “experimental” data points of $R_{\text{S}}(R_{\text{S}}^{\circ})^{-1}$ reported in the inset of Fig. 3. The solid curve in the same inset represents the rates predicted by considering the degradation of S by $^1\text{O}_2$, as well as the competition for $^1\text{O}_2$ between S and N_3^- . Such a curve was obtained by using the equivalent of eqn (7), with S instead of phenol and $k_{1\text{O}_2, \text{S}}$ assumed to be ten times higher than $k_{1\text{O}_2, \text{phenol}}$. In this case the $^1\text{O}_2$ curve is quite compatible with

the “experimental” data, which means that even small experimental errors would prevent the reactions with $^1\text{O}_2$ and with $^3\text{CBBP}^*$ to be distinguished by addition of NaN_3 .

FFA photodegradation. Differently from phenol, FFA undergoes important reaction with $^1\text{O}_2$ (the rate constant $k_{1\text{O}_2, \text{FFA}}$ is almost two orders of magnitude higher than $k_{1\text{O}_2, \text{phenol}}$)⁵⁰ and it is often used as a $^1\text{O}_2$ probe. Therefore, FFA is a suitable substrate to obtain indications about the possible involvement of $^1\text{O}_2$ in degradation processes induced by irradiated CBBP. The degradation rate of FFA (R_{FFA}) was studied as a function of FFA concentration, upon irradiation of $66 \mu\text{mol L}^{-1}$ CBBP. The experimental results are reported in Fig. 4 and they show a plateau trend with increasing FFA.

Considering that FFA reacts with $^3\text{CBBP}^*$ and with $^1\text{O}_2$, a suitable kinetic scheme should take both processes into account. The generation of $^1\text{O}_2$ by $^3\text{CBBP}^*$ involves the reaction between $^3\text{CBBP}^*$ and ground-state molecular oxygen. In an aerated solution containing CBBP alone, O_2 consumes approximately 68% of $^3\text{CBBP}^*$ as suggested by our LFP experiments. Therefore, one has $k_{3\text{CBBP}^*, \text{O}_2}[\text{O}_2] = 0.68k_2$. As one of the possible processes induced by the reaction between $^3\text{CBBP}^*$ and O_2 , the production of $^1\text{O}_2$ would account for a fraction, usually indicated as S_{Δ} , of the $^3\text{CBBP}^*$ quenching by O_2 . On this basis, the reaction scheme that describes the transformation of FFA in the presence of irradiated CBBP includes reactions (1) and (2) plus the following:

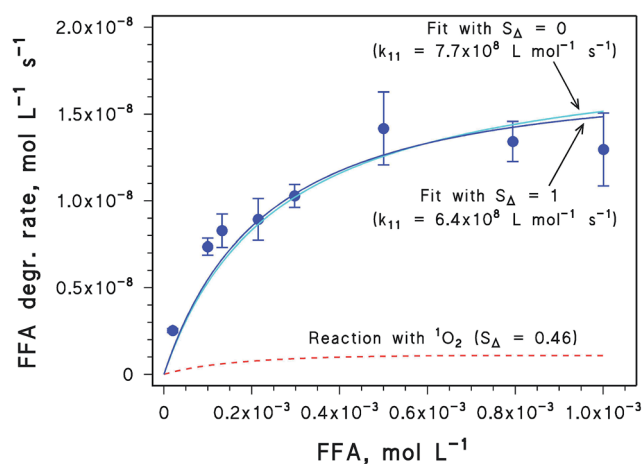
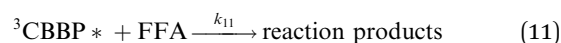
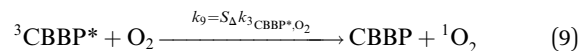
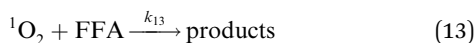


Fig. 4 Initial degradation rate of FFA (R_{FFA}) as a function of FFA concentration, upon irradiation in the presence of $66 \mu\text{mol L}^{-1}$ CBBP at $\text{pH} \sim 7$. The error bounds to the rate values ($\pm\sigma$) are derived from the fit of the time evolution data of FFA concentration. The light blue and blue solid curves represent the fit of the experimental data by eqn (14), with $S_{\Delta} = 0$ and $S_{\Delta} = 1$ (extreme values of S_{Δ}), respectively. The red dashed line represents the contribution of the $^1\text{O}_2$ reaction to FFA degradation if $S_{\Delta} = 0.46$, as assessed in this work.



Here, $k_{10} = 2.4 \times 10^9 \text{ L mol}^{-1} \text{ s}^{-1}$ is the total quenching rate constant of ${}^3\text{CBBP}^*$ by FFA determined by LFP (reaction (10), which also includes the actual reaction (11)), $k_{12} = k_d = 2.5 \times 10^5 \text{ s}^{-1}$ is the inactivation rate constant of ${}^1\text{O}_2$ in water,⁴⁴ and $k_{13} = 1.0 \times 10^8 \text{ L mol}^{-1} \text{ s}^{-1}$ is the reaction rate constant between FFA and ${}^1\text{O}_2$.⁵¹ The reaction between ${}^3\text{CBBP}^*$ and O_2 can be treated as a pseudo-first order process with a rate constant $k = k_{\text{CBBP}^*,\text{O}_2}[\text{O}_2] = 0.68k_2$. On this basis one obtains $k' = 0.68S_\Delta k_2$ as the pseudo-first order rate constant of ${}^1\text{O}_2$ formation by irradiated CBBP, where the ${}^1\text{O}_2$ formation rate is $R_{\text{O}_2} = k' [{}^3\text{CBBP}^*]$. By applying the steady-state approximation to ${}^3\text{CBBP}^*$ and ${}^1\text{O}_2$ one gets the following expression for R_{FFA} , where $R_{\text{CBBP}^*} = 5.8 \times 10^{-8} \text{ mol L}^{-1} \text{ s}^{-1}$ (see above) and all the other quantities are known except for k_{11} and S_Δ :

$$R_{\text{FFA}} = R_{\text{CBBP}^*} \left(\frac{k_{11}[\text{FFA}]}{k_2 + k_{10}[\text{FFA}]} + \frac{0.68S_\Delta k_2 k_{13}[\text{FFA}]}{(k_2 + k_{10}[\text{FFA}])(k_{12} + k_{13}[\text{FFA}])} \right) \quad (14)$$

Eqn (14) reproduces quite well the experimental data of R_{FFA} vs. $[\text{FFA}]$. In particular, the plateau trend can be accounted for quite precisely by the competition between ${}^3\text{CBBP}^*$ deactivation (reaction (2)) and quenching by FFA (reaction (10)). Differently from the case of phenol, there is hardly any need to invoke additional processes such as the back-reactions. Moreover, the relatively low value of the plateau $R_{\text{FFA}} \sim 1.5 \times 10^{-8} \text{ mol L}^{-1} \text{ s}^{-1}$ as compared to $R_{\text{CBBP}^*} = 5.8 \times 10^{-8} \text{ mol L}^{-1} \text{ s}^{-1}$ is largely accounted for by the fact that the reaction rate constant k_{11} is lower than the quenching rate constant k_{10} ($k_{11}k_{10}^{-1} \sim 0.3$, *vide infra*).

The fit calculations with eqn (14) of the experimental data reported in Fig. 4 initially used two free variables (k_{11} and S_Δ). In order to assess k_{11} from the fit of the experimental data reported in Fig. 4, one thus needs to fix the value of S_Δ that in principle may vary from 0 to 1.³⁵ All the relevant fit curves were very similar to one another: the two curves obtained with the extreme values $S_\Delta = 0$ and $S_\Delta = 1$ are shown in Fig. 4 as an example. However, it is highly unlikely that $S_\Delta = 1$, because aromatic carbonyls have relatively low efficiencies for ${}^1\text{O}_2$ generation.³⁴ Unfortunately, the formation of ${}^1\text{O}_2$ by ${}^3\text{CBBP}^*$ has never been quantified. Moreover, because of the significant reaction between FFA and ${}^3\text{CBBP}^*$, the present experimental data discourage the use of the molecular probe FFA to do it. The formation of ${}^1\text{O}_2$ has been measured in the case of benzophenone, by laser excitation and by monitoring of the IR fluorescence of ${}^1\text{O}_2$, obtaining $S_\Delta = 0.29$.³⁵ The different values of k_{11} that can be obtained by data fitting with eqn (14) are reported in Fig. 5, as a function of S_Δ . Because the formation rate of ${}^1\text{O}_2$ scales linearly with S_Δ , and the fit-derived k_{11} has to compensate for the presence or the absence of the ${}^1\text{O}_2$ reaction, the linear

trend of k_{11} vs. S_Δ is easily explained. We found $k_{11} \sim 7 \times 10^8 \text{ L mol}^{-1} \text{ s}^{-1}$ that is lower than k_{10} , as anticipated. The uncertainty on S_Δ translates into an uncertainty on k_{11} ; however, the extreme values of k_{11} , obtained with $S_\Delta = 0$ and with $S_\Delta = 1$, differ by approximately 17% that is not much higher than the experimental errors.

To be more precise in these determinations, one has to assess the role of ${}^1\text{O}_2$ in FFA degradation. To do so, and to obtain S_Δ as a consequence, we carried out irradiation experiments of FFA + CBBP in D_2O vs. H_2O as the solvent, under otherwise identical conditions (see Fig. ESI8†). The degradation rate of FFA in D_2O was double compared to that in H_2O . Considering that the first-order decay constant of ${}^1\text{O}_2$ in D_2O ($2 \times 10^4 \text{ s}^{-1}$) is 12.5 times lower than that in H_2O ($k_{12} = 2.5 \times 10^5 \text{ s}^{-1}$),⁵⁰ and because there is no reason to believe that the formation rate of ${}^1\text{O}_2$ in D_2O may be different from that in H_2O , one has $[{}^1\text{O}_2]_{\text{D}_2\text{O}} = 12.5[{}^1\text{O}_2]_{\text{H}_2\text{O}}$. The degradation of FFA in both systems would be accounted for by a combination of reaction (11) with ${}^3\text{CBBP}^*$ (with the quenching process (10) also being operational) and reaction (13) with ${}^1\text{O}_2$. Again, there is no reason to believe that k_{10} , k_{11} , k_{13} or $[{}^3\text{CBBP}^*]$ may be different in D_2O compared to H_2O , and the only reasonable difference between the two systems is thus $[{}^1\text{O}_2]$. Therefore, in order to account for the doubling of FFA degradation kinetics in D_2O compared to H_2O , in the H_2O solvent only 9.5% FFA should be degraded by ${}^1\text{O}_2$, while the remaining 90.5% FFA would be degraded by ${}^3\text{CBBP}^*$. In other words, the contribution of ${}^3\text{CBBP}^*$ to FFA degradation in H_2O (which is also represented by the left-hand-side term of the sum in eqn (14), an equation that represents $R_{\text{FFA}} = R_{\text{FFA},\text{H}_2\text{O}}^{\text{CBBP}^*} + R_{\text{FFA},\text{H}_2\text{O}}^{\text{O}_2}$) should be 9.5 times higher than that of ${}^1\text{O}_2$ (right-hand-side term). Therefore, one has $\xi = R_{\text{FFA},\text{H}_2\text{O}}^{\text{CBBP}^*} (R_{\text{FFA},\text{H}_2\text{O}}^{\text{O}_2})^{-1} = 9.5$. Upon application of this result to eqn (14) one gets the following expression for S_Δ :

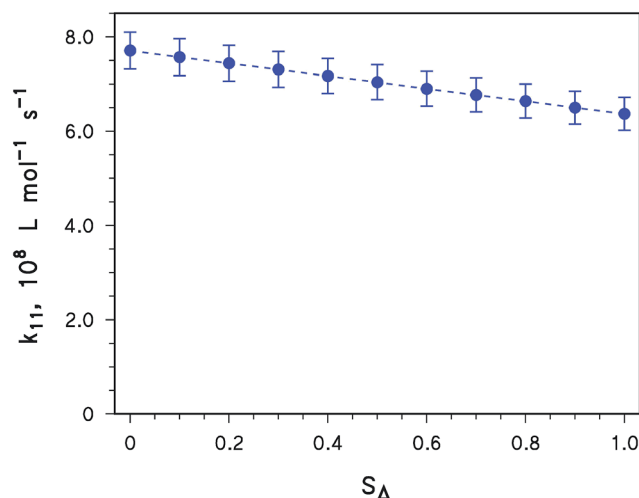


Fig. 5 Values of k_{11} derived from the fit with eqn (14) of the experimental data shown in Fig. 4, as a function of S_Δ that is the efficiency of ${}^1\text{O}_2$ production in the quenching of ${}^3\text{CBBP}^*$ by O_2 . The error bounds ($\pm\sigma$) represent the fit uncertainty. The dashed line is just a guide for the eye.

$$S_{\Delta} = \frac{k_{11}(k_{12} + k_{13}[\text{FFA}])}{0.68\xi k_2 k_{13}} \quad (15)$$

Note that S_{Δ} and k_{11} are to be obtained by fitting the same experimental data, and thus they are not totally independent variables. However, with sequential adjustments carried out with multiple data fits one gets $S_{\Delta} = 0.46$ and $k_{11} = 7 \times 10^8 \text{ L mol}^{-1} \text{ s}^{-1}$. We assessed the FFA transformation rate, accounted for by $^1\text{O}_2$, by using eqn (14) deprived of the first term in parentheses that depends on the $^3\text{CBBP}^*$ reactivity, with $S_{\Delta} = 0.46$. The results are reported in Fig. 4 and they show that singlet oxygen would only play a secondary role in FFA degradation. Interestingly, even by assuming the most favourable conditions to $^1\text{O}_2$ reactions ($S_{\Delta} = 1$), most of the FFA degradation would still be accounted for by $^3\text{CBBP}^*$.

Additional evidence for a limited role of $^1\text{O}_2$ in the degradation of FFA sensitised by CBBP was obtained by means of further irradiation experiments, coupled with GC-MS runs to identify the phototransformation intermediates (see the ESI for further details, Fig. ESI9–13†). Furfural was the only detected FFA transformation intermediate (trace benzaldehyde was also detected, but it likely derives from the transformation of CBBP). Furfural is formed upon FFA oxidation⁵² and in our experiments it also occurred in a small amount in the initial FFA, but its concentration increased considerably during irradiation (the formation yield of furfural from FFA would be almost quantitative according to our data). In contrast, 6-hydroxy(2*H*)pyran-3(6*H*)-one that is the product of the reaction between FFA and $^1\text{O}_2$ (ref. 23) could not be detected (the detection limit for the compounds analysed by GC-MS was here around $0.1 \mu\text{mol L}^{-1}$). The formation of furfural is consistent with a major oxidative process of FFA phototransformation induced by $^3\text{CBBP}^*$, without an important role of $^1\text{O}_2$.

Coherently with the above findings, the degradation kinetics of FFA in the presence of irradiated CBBP was affected by the occurrence of oxygen in the overlying atmosphere. Because dissolved O_2 would scavenge $^3\text{CBBP}^*$, thereby inhibiting the degradation of FFA, one observes the following order in the transformation rate of FFA: pure $\text{N}_2 > \text{air} > \text{pure } \text{O}_2$ (see ESI, Fig. ESI14†). If transformation of FFA by $^1\text{O}_2$ prevailed, one would expect the reverse order to be observed.

Validity of $^3\text{CBBP}^*$ as a $^3\text{CDOM}^*$ proxy

The reaction rate constant between $^3\text{CBBP}^*$ and phenol determined here ($(6.4 \pm 0.3) \times 10^8 \text{ L mol}^{-1} \text{ s}^{-1}$) is in the same range as the typical reaction rate constants between $^3\text{CDOM}^*$ and phenolic compounds,^{6,7,23} which looks favourable for the use of $^3\text{CBBP}^*$ as a $^3\text{CDOM}^*$ proxy. Also note that a reasonable agreement between $^3\text{CBBP}^*$ and $^3\text{CDOM}^*$ reactivity has been reported in the case of diclofenac as well.²⁰ By comparison, the reaction rate constant between $^3\text{AQ2S}^*$ and phenol is above $3 \times 10^9 \text{ L mol}^{-1} \text{ s}^{-1}$.⁵³ The measured reaction rate constant between $^3\text{CBBP}^*$ and FFA ($7 \times 10^8 \text{ L mol}^{-1} \text{ s}^{-1}$) deserves some comment. On the one hand the similarity with

the phenol rate constant may be reasonable (FFA and phenol have also very similar reaction rate constants to ^1OH),⁵⁴ but on the other hand one should consider the similarities and differences in behaviour between $^3\text{CBBP}^*$ and $^3\text{CDOM}^*$. Note that $^3\text{CBBP}^*$ and $^3\text{CDOM}^*$ have very similar deactivation rate constants in aerated solution: $6 \times 10^5 \text{ s}^{-1}$ ($^3\text{CBBP}^*$, this work) vs. $\sim 5 \times 10^5 \text{ s}^{-1}$ ($^3\text{CDOM}^*$), and also the value of $S_{\Delta} = 0.46$ for the $^1\text{O}_2$ yield of $^3\text{CBBP}^*$ is not very far from the $^3\text{CDOM}^*$ range of S_{Δ} values.⁷ Therefore, the ratio of the steady-state $[\text{O}_2] [\text{CBBP}^*]^{-1}$ (around 1 with CBBP alone) in our experimental systems should be not far from the typical ratios of $[\text{O}_2] [\text{CDOM}^*]^{-1}$ that are found upon irradiation of natural water samples.⁷ From this point of view, irradiated CBBP has the potential to produce $^1\text{O}_2$ to a significant extent. However, FFA with irradiated humic substances is reported to mainly react with $^1\text{O}_2$,²³ while in our case it was shown to mainly react with $^3\text{CBBP}^*$. This difference can be accounted for in two alternative ways: (i) the reaction between FFA and $^3\text{CBBP}^*$ is much faster than the reaction between FFA and $^3\text{CDOM}^*$ (in which case, $^3\text{CBBP}^*$ would not be a good $^3\text{CDOM}^*$ proxy in the case of FFA), or (ii) this result is due to the large difference between the quenching rate constant of $^3\text{CBBP}^*$ with FFA and the corresponding reaction rate constant. The elevated quenching rate constant could cause inactivation of $^3\text{CBBP}^*$ by FFA (even without net reaction) and inhibit the ability of the triplet state to produce $^1\text{O}_2$ (thereby giving $[\text{O}_2] [\text{CBBP}^*]^{-1} < 1$). The same would probably not occur with $^3\text{CDOM}^*$, as the FFA quenching rate constant is unlikely to be that high. A third alternative explanation questions the ability of FFA to probe $^1\text{O}_2$ in irradiated CDOM solutions. It is clear that additional work is needed to understand whether and to what extent the good performance of $^3\text{CBBP}^*$ as a $^3\text{CDOM}^*$ proxy, highlighted in the cases of phenol and diclofenac, can be extended to other xenobiotic compounds.

A protocol for the measurement of the $^3\text{CBBP}^*$ rate constants

Assume a generic molecule M that reacts with $^3\text{CBBP}^*$, with the quenching constant $k_{\text{CBBP}^*,\text{M}}^{\text{O}}$ and the reaction rate constant $k_{\text{CBBP}^*,\text{M}}^{\text{R}}$. As before, one has $k_{\text{CBBP}^*,\text{M}}^{\text{R}} \leq k_{\text{CBBP}^*,\text{M}}^{\text{O}}$. One needs to preliminarily know the reaction rate constant between M and $^1\text{O}_2$, $k_{\text{O}_2,\text{M}}$, which can be measured quite easily by using a suitable $^1\text{O}_2$ source such as Rose Bengal.^{14,24} To measure $k_{\text{CBBP}^*,\text{M}}^{\text{R}}$, one has to determine the degradation rate of M (R_{M}) in the presence of CBBP under steady-state irradiation, as a function of M concentration. Note that neither phenol nor FFA underwent direct photolysis under our irradiation set-up, but this possibility cannot be excluded in the most general case. If applicable, the rate of M direct photolysis in the presence of CBBP ($R_{\text{phot},\text{M}}^{\text{CBBP}}$) is proportional to the photon flux absorbed by M, which depends on the competition for irradiance between M and CBBP. By knowing the direct photolysis rate of M when alone in solution ($R_{\text{phot},\text{M}}$) and the absorption spectra of both M and CBBP, one can obtain $R_{\text{phot},\text{M}}^{\text{CBBP}}$ from $R_{\text{phot},\text{M}}$ by the following equation:^{13,41}

$$R_{\text{phot},M}^{\text{CBBP}} = R_{\text{phot},M} \frac{\int_{\lambda} p^{\circ}(\lambda) \frac{\varepsilon_{\text{M}}(\lambda)[\text{M}]}{\varepsilon_{\text{CBBP}}(\lambda)[\text{CBBP}] + \varepsilon_{\text{M}}(\lambda)[\text{M}]} [1 - 10^{-b(\varepsilon_{\text{CBBP}}(\lambda)[\text{CBBP}] + \varepsilon_{\text{M}}(\lambda)[\text{M}])}] d\lambda}{\int_{\lambda} p^{\circ}(\lambda) [1 - 10^{-\varepsilon_{\text{M}}(\lambda)b[\text{M}]}] d\lambda} \quad (16)$$

where $p^{\circ}(\lambda)$ is the incident spectral photon flux density of the lamp, $\varepsilon_{\text{M}}(\lambda)$ and $\varepsilon_{\text{CBBP}}(\lambda)$ are the molar absorption coefficients of M and CBBP, respectively, and b is the optical path length inside the irradiated solution. A comparable kinetic model to that already developed for FFA yields the following result for R'_{M} (degradation rate of M after subtraction of $R_{\text{phot},M}^{\text{CBBP}}$) vs. [M]:

$$R'_{\text{M}} = R_{\text{CBBP}^*} \left(\frac{k_{\text{CBBP}^*,\text{M}}^{\text{R}}[\text{M}]}{k_2 + k_{\text{CBBP}^*,\text{M}}^{\text{Q}}[\text{M}]} + \frac{0.68S_{\Delta}k_2k_{\text{O}_2,\text{M}}[\text{M}]}{(k_2 + k_{\text{CBBP}^*,\text{M}}^{\text{Q}}[\text{M}])(k_{12} + k_{\text{O}_2,\text{M}}[\text{M}])} \right) \quad (17)$$

Note that $R_{\text{CBBP}^*} = \Phi_{\text{CBBP}^*}^{\text{CBBP}} P_{\text{a}}^{\text{CBBP}} = P_{\text{a}}^{\text{CBBP}}$. Some issues with eqn (17) have to be highlighted. First of all, one needs a LFP apparatus to determine $k_{\text{CBBP}^*,\text{M}}^{\text{Q}}$, which is not acceptable for a protocol that should work with steady-state irradiation alone. Moreover, if M behaved in a similar way to phenol, and differently from FFA, the equation would not fit well the experimental data because it does not take into account additional processes, e.g., the possible back-reactions between the radical species formed by $^3\text{CBBP}^*$ and M. Both issues can be circumvented if one limits the examination of the R'_{M} vs. [M] data to the linear part that is obtained at low [M]. In this case the experimental data have the form of $R'_{\text{M}} = m[\text{M}]$, where m is the line slope. A linear trend can be foreseen by eqn (17) if $k_{\text{CBBP}^*,\text{M}}^{\text{Q}}[\text{M}] \ll k_2$ and if $k_{\text{O}_2,\text{M}}[\text{M}] \ll k_{12}$. Therefore, if one observes a linear trend in the experimental data (or if one concentrates on the linear part of the experimental data), the $k_{\text{CBBP}^*,\text{M}}^{\text{Q}}[\text{M}]$ term in eqn (17) can be excluded as negligible and one does not need to assess $k_{\text{CBBP}^*,\text{M}}^{\text{Q}}$ by LFP. Moreover, processes such as the back reactions can be neglected if they are unable to shift the experimental data away from a linear trend.⁴⁵ From the comparison between the linearised form of eqn (17) and the experimental data, one can obtain the rate constant $k_{\text{CBBP}^*,\text{M}}^{\text{R}}$ as follows:

$$k_{\text{CBBP}^*,\text{M}}^{\text{R}} = k_2 \left(\frac{m}{R_{\text{CBBP}^*}} - \frac{0.68S_{\Delta}k_{\text{O}_2,\text{M}}}{k_{12}} \right) \quad (18)$$

where $R_{\text{CBBP}^*} = P_{\text{a}}^{\text{CBBP}}$, $k_2 = 6 \times 10^5 \text{ s}^{-1}$, $k_{12} = 2.5 \times 10^5 \text{ s}^{-1}$ (ref. 44) and $S_{\Delta} = 0.46$ (this work). Note that eqn (18) does not contain LFP-derived $k_{\text{CBBP}^*,\text{M}}^{\text{Q}}$. This means that, with the approach we are describing, one does not need a LFP apparatus to determine $k_{\text{CBBP}^*,\text{M}}^{\text{R}}$: a (low-cost) steady-state irradiation set-up and a liquid chromatograph (or other suitable analytical equipment) is all what one needs. In the most general case, when M absorbs radiation, $P_{\text{a}}^{\text{CBBP}}$ (and $R_{\text{CBBP}^*} = P_{\text{a}}^{\text{CBBP}}$ as a consequence) can be calculated as follows:

$$P_{\text{a}}^{\text{CBBP}} = \int_{\lambda} p^{\circ}(\lambda) \frac{\varepsilon_{\text{CBBP}}(\lambda)[\text{CBBP}]}{\varepsilon_{\text{CBBP}}(\lambda)[\text{CBBP}] + \varepsilon_{\text{M}}(\lambda)[\text{M}]} \times [1 - 10^{-b(\varepsilon_{\text{CBBP}}(\lambda)[\text{CBBP}] + \varepsilon_{\text{M}}(\lambda)[\text{M}])}] d\lambda \quad (19)$$

Conclusions

An argument in favour of the use of CBBP as a CDOM proxy for the measurement of the reaction rate constants of triplet sensitisation is the sufficiently similar reactivity between $^3\text{CBBP}^*$ and $^3\text{CDOM}^*$.²⁰ The rate constants of $^3\text{CBBP}^*$ quenching by organic compounds can be easily measured by LFP, but they are not necessarily representative of the actual reaction rate constants. Indeed, the one-electron abstraction by $^3\text{CBBP}^*$ on a molecule M would yield the reduced form $\text{CBBP}^{\cdot-}$ that tends to form an ion couple with $\text{M}^{\cdot+}$, partially giving back CBBP and M.²⁸ This is the likely reason for which, in the cases of both phenol and FFA in this work, we obtained reaction rate constants with $^3\text{CBBP}^*$ that were significantly lower than the quenching rate constants measured by LFP.

In the case of FFA we could define a kinetic model able to reproduce the trend of R_{FFA} vs. [FFA] under steady-state irradiation conditions, including the plateau at high [FFA]. This kinetic model, however, requires the knowledge of the quenching rate constant $k_{\text{CBBP}^*,\text{S}}^{\text{Q}}$ obtained in LFP experiments. In the case of phenol the plateau trend of the degradation rate was presumably due to additional reactions (e.g., back reactions). In particular, the back reaction between phenoxyl and superoxide allowed a (quite complex) kinetic equation to be obtained with some approximations, which correctly predicted the observed plateau. The problems connected with quenching rate constants and additional reactions can be avoided by operating at sufficiently low substrate concentration, where a linear trend of the degradation rate vs. concentration can be observed.

A further potential problem was the previously unknown formation rate of $^1\text{O}_2$ by irradiated CBBP, which produces an uncertainty in the determination of the $^3\text{CBBP}^*$ reaction rate constants. By means of irradiation experiments in H_2O and D_2O , we were able to assess $S_{\Delta} = 0.46$ as the $^1\text{O}_2$ yield of the quenching reaction between $^3\text{CBBP}^*$ and O_2 . Remarkably, $^3\text{CBBP}^*$ is quenched fast (quenching constants above $10^9 \text{ L mol}^{-1} \text{ s}^{-1}$) by FFA and azide that are typically used as a $^1\text{O}_2$ probe and quencher, respectively. Therefore, we do not recommend the use of probes/quenchers to obtain mechanistic information on systems containing CBBP under irradiation.

Here we were able to demonstrate that the degradation of FFA mainly took place upon reaction with $^3\text{CBBP}^*$ and that $^1\text{O}_2$ played a minor role in the process. This is a good finding because it excludes the risk of $^1\text{O}_2$ interference in the measurement of the $^3\text{CBBP}^*$ reaction rate constants, even in the

presence of compounds that react fast with $^1\text{O}_2$. However, this may also have implications either on the ability of $^3\text{CBBP}^*$ to be a good $^3\text{CDOM}^*$ proxy in the case of FFA or on the ability of FFA to probe $^1\text{O}_2$ in the presence of irradiated CDOM. This issue clearly deserves additional investigation.

Based on the above considerations, a protocol can be proposed for the measurement of the reaction rate constant of a generic molecule M in the presence of $^3\text{CBBP}^*$. The protocol works as follows: (i) preliminarily measure or find in the literature the reaction rate constant between M and $^1\text{O}_2$; (ii) study the rate R_M induced by irradiated CBBP and detect the conditions at low [M] where the trend of R_M vs. [M] is linear; (iii) if applicable, account for the direct photolysis of M by subtracting the direct photolysis rate from R_M to obtain R'_M ; (iv) determine the slope m of the R'_M vs. [M] line; (v) use eqn (18) to obtain the reaction rate constant $k_{^3\text{CBBP}^*,\text{S}}^R$ ($S_\Delta = 0.46$), calculating $R_{^3\text{CBBP}^*} = P_a^{\text{CBBP}}$ with eqn (19).

Conflicts of interest

There are no conflicts to declare.

Acknowledgements

DV and MM acknowledge financial support by MIUR-PNRA (contract PNRA14_00026). MB thanks University Clermont Auvergne for the visiting professor programme provided to MM.

References

- 1 K. Fenner, S. Canonica, L. P. Wackett and M. Elsner, *Science*, 2013, **341**, 752–758.
- 2 A. Pace and S. Barreca, *Curr. Org. Chem.*, 2013, **17**, 3032–3041.
- 3 T. Kutser, D. Pierson, L. Tranvik, A. Reinart, S. Sobek and K. Kallio, *Ecosystems*, 2005, **8**, 709–720.
- 4 P. H. Li and J. Hur, *Crit. Rev. Environ. Sci. Technol.*, 2017, **47**, 131–154.
- 5 D. Vione, M. Minella, V. Maurino and C. Minero, *Chem.–Eur. J.*, 2014, **20**, 10590–10606.
- 6 F. L. Rosario-Ortiz and S. Canonica, *Environ. Sci. Technol.*, 2016, **50**, 12532–12547.
- 7 K. McNeill and S. Canonica, *Environ. Sci.: Processes Impacts*, 2016, **18**, 1381–1399.
- 8 R. Cory and D. McKnight, *Environ. Sci. Technol.*, 2005, **39**, 8142–8149.
- 9 C. M. Sharpless, *Environ. Sci. Technol.*, 2012, **46**, 4466–4473.
- 10 K. Golanoski, S. Fang, R. Del Vecchio and N. V. Blough, *Environ. Sci. Technol.*, 2012, **46**, 3912–3920.
- 11 C. M. Sharpless and N. V. Blough, *Environ. Sci.: Processes Impacts*, 2014, **16**, 654–671.
- 12 E. De Laurentiis, M. Minella, V. Maurino, C. Minero, M. Brigante, G. Mailhot and D. Vione, *Chemosphere*, 2012, **88**, 1208–1213.
- 13 M. Bodrato and D. Vione, *Environ. Sci.: Processes Impacts*, 2014, **16**, 732–740.
- 14 E. De Laurentiis, C. Prasse, T. A. Ternes, M. Minella, V. Maurino, C. Minero, M. Sarakha, M. Brigante and D. Vione, *Water Res.*, 2014, **53**, 235–248.
- 15 P. Calza, G. Noé, D. Fabbri, V. Santoro, C. Minero, D. Vione and C. Medana, *Water Res.*, 2017, **122**, 194–206.
- 16 A. E. Hartenbach, T. B. Hofstetter, P. R. Tentscher, S. Canonica, M. Berg and R. P. Schwarzenbach, *Environ. Sci. Technol.*, 2008, **42**, 7751–7756.
- 17 J. Wenk, S. N. Eustis, K. McNeill and S. Canonica, *Environ. Sci. Technol.*, 2013, **47**, 12802–12810.
- 18 S. Canonica, B. Hellrung and J. Wirz, *J. Phys. Chem. A*, 2000, **104**, 1226–1232.
- 19 S. Canonica, B. Hellrung, P. Mueller and J. Wirz, *Environ. Sci. Technol.*, 2006, **40**, 6636–6641.
- 20 P. Avetta, D. Fabbri, M. Minella, M. Brigante, V. Maurino, C. Minero, M. Pazzi and D. Vione, *Water Res.*, 2016, **105**, 383–394.
- 21 P. R. Maddigapu, A. Bedini, C. Minero, V. Maurino, D. Vione, M. Brigante, G. Mailhot and M. Sarakha, *Photochem. Photobiol. Sci.*, 2010, **9**, 323–330.
- 22 A. Bedini, E. De Laurentiis, B. Sur, V. Maurino, C. Minero, M. Brigante, G. Mailhot and D. Vione, *Photochem. Photobiol. Sci.*, 2012, **11**, 1445–1453.
- 23 S. Halladja, A. Ter Halle, J. P. Aguer, A. Boulkamh and C. Richard, *Environ. Sci. Technol.*, 2007, **41**, 6066–6073.
- 24 G. Marchetti, M. Minella, V. Maurino, C. Minero and D. Vione, *Water Res.*, 2013, **47**, 6211–6222.
- 25 T. Zeng and A. Arnold, *Environ. Sci. Technol.*, 2013, **47**, 6735–6745.
- 26 Y. J. Li, X. X. Wei, J. W. Chen, H. B. Xie and Y. N. Zhang, *J. Hazard. Mater.*, 2015, **290**, 9–15.
- 27 P. Filipiak, K. Bobrowski, G. L. Hug, D. Pogocki, C. Schöneich and B. Marciniak, *J. Phys. Chem. B*, 2017, **121**, 5247–5258.
- 28 J. K. Hurley, H. Linschitz and A. Treinin, *J. Phys. Chem.*, 1988, **92**, 5151–5159.
- 29 R. M. Smith, A. E. Martell and R. J. Motekaitis, *NIST Critical Selected Stability Constant of Metal Complexes Database 46 (Version 6.0)*, 2001.
- 30 A. Marchisio, M. Minella, V. Maurino, C. Minero and D. Vione, *Water Res.*, 2015, **73**, 145–156.
- 31 I. Zebger, J. W. Snyder, L. K. Andersen, L. Poulsen, Z. Gao, D. C. John, U. Kristiansen, P. R. Ogilby and J. D. C. Lambert, *Photochem. Photobiol.*, 2004, **79**, 319–322.
- 32 B. Marciniak, K. Bobrowski, G. L. Hug and J. Rozwadowski, *J. Phys. Chem.*, 1994, **98**, 4854–4860.
- 33 E. De Laurentiis, J. Socorro, D. Vione, E. Quivet, M. Brigante, G. Mailhot, H. Wortham and S. Gligorovski, *Atmos. Environ.*, 2013, **81**, 569–578.
- 34 A. A. Gorman, G. Lovering and M. A. J. Rodgers, *J. Am. Chem. Soc.*, 1978, **100**, 4527–4532.
- 35 A. A. Gorman, I. Hamblett and M. A. J. Rodgers, *J. Am. Chem. Soc.*, 1984, **106**, 4679–4682.
- 36 M. Bancirova, *Luminescence*, 2011, **26**, 685–688.
- 37 J. Brame, M. Long, Q. Li and P. Alvarez, *Water Res.*, 2014, **60**, 259–266.

- 38 M. Gmurek, M. Olak-Kucharczyk and S. Ledakowicz, *J. Environ. Health Sci. Eng.*, 2015, **13**, 28.
- 39 Z. B. Alfassi, A. Harriman, R. E. Huie, S. Mosseri and P. Neta, *J. Phys. Chem.*, 1987, **91**, 2120–2122.
- 40 K. J. Kim, H.-C. Kim, M. Park and S. Huh, *Appl. Surf. Sci.*, 2017, **414**, 325–334.
- 41 S. E. Braslavsky, *Pure Appl. Chem.*, 2007, **79**, 293–465.
- 42 P. G. Tratnyek and J. Hoigné, *Environ. Sci. Technol.*, 1991, **25**, 1596–1604.
- 43 C. Li and M. Z. Hoffman, *J. Phys. Chem. A*, 2000, **104**, 5998–6002.
- 44 M. A. J. Rodgers and P. T. Snowden, *J. Am. Chem. Soc.*, 1982, **104**, 5541–5543.
- 45 C. Minero, *Catal. Today*, 1999, **54**, 205–216.
- 46 L. R. Mahoney and S. A. Weiner, *J. Am. Chem. Soc.*, 1972, **94**, 585–590.
- 47 D. R. Armstrong, C. Cameron, D. C. Nonhebel and P. G. Perkins, *J. Chem. Soc., Perkin Trans. 2*, 1983, 587–589.
- 48 P. Neta and J. Grodkowski, *J. Phys. Chem. Ref. Data*, 2005, **34**, 109–199.
- 49 W. R. Haag and T. Mill, *Photochem. Photobiol.*, 1987, **45**, 317–321.
- 50 F. Wilkinson, W. P. Helman and A. B. Ross, *J. Phys. Chem. Ref. Data*, 1995, **24**, 663–1021.
- 51 E. Appiani, R. Ossola, D. E. Latch, P. R. Erickson and K. McNeill, *Environ. Sci.: Processes Impacts*, 2017, **19**, 507–516.
- 52 R. Bensasson and E. J. Land, *Photochem. Photobiol. Rev.*, 1978, **3**, 163–191.
- 53 V. Maurino, D. Borghesi, D. Vione and C. Minero, *Photochem. Photobiol. Sci.*, 2008, **7**, 321–327.
- 54 G. V. Buxton, C. L. Greenstock, W. P. Helman and A. B. Ross, *J. Phys. Chem. Ref. Data*, 1988, **17**, 513–886.